Journal of Computer-Aided Molecular Design, **15:** 381–393, 2001.
KLUWER/ESCOM

Very empirical treatment of solvation and entropy: a force field derived from Log $P_{o/w}$

Glen Eugene Kellogg*, James C. Burnett & Donald J. Abraham
Institute for Structural Biology and Drug Discovery & Department of Medicinal Chemistry, School of Pharmacy, Virginia Commonwealth University, Richmond, VA 23298-0133 USA

Received 10 August 2000; accepted 23 October 2000

Key words: desolvation energy, dihydrofolate reductase, free energy of association, HINT, hydropathic interactions, hydrophobicity, methotrexate, molecular modeling

Summary

A non-covalent interaction force field model derived from the partition coefficient of 1-octanol/water solubility is described. This model, HINT for Hydropathic INTeractions, is shown to include, in very empirical and approximate terms, all components of biomolecular associations, including hydrogen bonding, Coulombic interactions, hydrophobic interactions, entropy and solvation/desolvation. Particular emphasis is placed on: (1) demonstrating the relationship between the total empirical HINT score and free energy of association, $\Delta G_{\text{interaction}}$; (2) showing that the HINT hydrophobic-polar interaction sub-score represents the energy cost of desolvation upon binding for interacting biomolecules; and (3) a new methodology for treating constrained water molecules as discrete independent small ligands. An example calculation is reported for dihydrofolate reductase (DHFR) bound with methotrexate (MTX). In that case the observed very tight binding, $\Delta G_{\text{interaction}} \leq -13.6$ kcal mol^{-1}, is largely due to ten hydrogen bonds between the ligand and enzyme with estimated strength ranging between -0.4 and -2.3 kcal mol^{-1}. Four water molecules bridging between DHFR and MTX contribute an additional -1.7 kcal mol^{-1} stability to the complex. The HINT estimate of the cost of desolvation is $+13.9$ kcal mol^{-1}.

Introduction

As our efforts to discover, design and develop new therapeutic agents accelerate, our desire to more thoroughly understand the biomolecular environment increasingly relies upon an appreciation of chemical structure and chemical interactions. For large biological molecules structure and interactions are intimately related. It is not enough to know the 'bonded' structure; it is also mandatory to understand the non-covalent interactions that lead to gross macromolecular structure. It is these effects that produce the binding sites, pockets, clefts and etc. that are the targets for structure-based drug discovery. As if this is not difficult enough, nature has added another factor in the biological environment that adds considerable complexity. This is, of course, the omnipresent water molecules that affect these associations directly by mediating hydrogen bonding, indirectly by driving the hydrophobic effect, and even more indirectly by influencing entropic changes in the system through the gain or loss of water 'structure' [1]. All of these associations and interactions are key to understanding biological action at the molecular level.

Technological forces are responsible for much of the increasing utilization of this structural biology paradigm. The rapidly growing availability [2] of experimental three-dimensional structural data for macromolecules (proteins, enzymes, nucleic acids, etc.) from crystallography and multidimensional NMR, combined with the exponential increase in the power and sophistication of computer hardware and software, provides an unprecedented ability to visualize biological macromolecular structure. From this visualization comes the ability to rationally design inhibitors, site-

*To whom correspondence should be addressed. E-mail: Glen.Kellogg@vcu.edu

directed mutations or other chemical changes that lead to biological effects.

While quantum analytical methods can be used to gain a very detailed comprehension of the electronic structure and properties of small molecules, they cannot yet be applied to even modestly-sized biological macromolecules. However, molecular mechanics can be reasonably and accurately applied to many structural/geometry optimization problems in the biological environment. Thus it is possible to predict the 3D structure of small molecules, examine the dynamics of protein and nucleotide structure [3] and study the docking interactions of small molecule-macromolecule complexes [4]. Molecular mechanics 'force fields' include intramolecular (bonded) terms for bond stretches, angle bending, and torsions, and (non-bonded) terms for Coulombic, Van der Waals, and hydrogen bonding interactions.

In small molecules and within small pieces of macromolecules the 'bonded' terms are dominant and molecular mechanics does a very good job of predicting the structure because these functions are relatively simple and very easy to verify. Non-bonded terms, however, are not as well understood or functionalized and are the ones affecting the structural features and motifs that are, for example in proteins, termed secondary, tertiary, and quaternary structure. In fact, it is counterintuitive that so much of the fine structural detail of a protein can be so *well* predicted when the gross structural features are so *poorly* reproduced. Very significant is that molecular mechanics methods do not include any terms for estimating entropic energy. Likewise, solvation/desolvation is not explicitly treated in commonly used molecular mechanics methods.

One commonly accepted non-covalent, entropically-driven, interaction important in the biological environment arises from hydrophobicity. Hydrophobicity and hydrophobic interaction forces are missing components of molecular mechanics. Clearly the term 'hydrophobic bonding' is a misnomer; however, there *is* an associated effect whereby hydrophobic entities tend to congregate and exclude water [5]. While the driving force for this hydrophobic effect likely stems from the formation of a network of hydrogen bonds among the water and polar groups of the system, i.e., the hydrophobic effect is an observed consequence and not really a force, we will show in this report that there is significant value in treating the hydrophobic effect as a real and *primary* phenomenon.

Structural biologists and others have debated the hydrophobic effect for decades [6]. Its influence on protein folding and other structural features is uniformly accepted, but rationalizing this influence has been difficult. A variety of scales for relative amino acid side chain hydrophobicities have been proposed, and these have been used fairly successfully for protein secondary structure prediction [7]. However, these data and this paradigm do not address hydrophobic interactions directly or quantitatively. In contrast, medicinal chemists, working with small molecules, have developed a rich understanding of hydrophobicity and hydrophobic interactions. Largely through the efforts of Corwin Hansch, Al Leo and the Pomona College MedChem Project [8], a remarkable collection of hydrophobicity data for many thousands of drugs and drug-like substances has been accumulated and made available to the community. Hydrophobicity is usually reported as $\mathrm{Log\,P_{o/w}}$, the $\mathrm{Log_{10}}$ of the partition coefficient for 1-octanol/water solubility. Hydrophobicity turns out to be a very important predictor of drug activity, particularly in cases where membrane transport is significant [9]. From the Pomona data base numerous models have been created to predict $\mathrm{Log\,P_{o/w}}$ based on the structures of small molecules. This aspect has been reviewed elsewhere [10]. Our work, in developing a modeling approach we call HINT (for Hydropathic INTeractions) [11–16], has focused on exploiting the thermodynamic information encoded in $\mathrm{Log\,P_{o/w}}$ to describe the hydrophobic effect, ligand solvation and desolvation energy, and other non-covalent forces as they effect biomolecular associations.

Our idea is actually very simple: each atom in a molecule has an interaction propensity based on its partial (atomic) $\mathrm{Log\,P_{o/w}}$ which we call a_i, the hydrophobic atom constant. This is, of course, by analogy to f_n, the hydrophobic fragment constant described by Hansch and Leo [17]. We use a simple approach to calculate the set of a_i from f_n that incorporates the important inter-fragment factors, retains the relation $\Sigma\ a_i = \mathrm{Log\,P_{o/w}}$, and emphasizes the importance of 'mantle' or 'frontier' atoms of the fragment(s) over buried atoms [13]. One of the overriding goals of *all* of the features of HINT is that we use the $\mathrm{Log\,P_{o/w}}$ data as directly and unprocessed as possible in the model by using simple methodology to calculate the HINT parameters. In the paragraphs below we will show the richness of thermodynamic information in this set of hydrophobic atom constants.

The HINT model

HINT is an intuitive and natural free energy force field based on $\mathrm{Log\,P_{o/w}}$ which experimentally measures interactions between molecules and the two solvents. Thus, the effects of entropy and solvation should be automatically part of the derived interactions as are hydrogen bonding, Coulombic, acid-base and hydrophobic associations. These factors are all consequential to understanding biological structure and developing strategies for drug discovery. HINT uses the experimental data from solvent partitioning experiments, $\mathrm{Log\,P_{o/w}}$ as described above, for interaction classification and quantitative scoring. The HINT model for biomolecular interactions includes all noncovalent interactions because all are manifested in one way or another in the experimental measurement of $\mathrm{Log\,P_{o/w}}$. Hydropathy is a term which refers to hydrophobic and polar interactions collectively [18]. In HINT hydropathic attractions between species, including hydrogen-bonding, acid-base interactions, Coulombic attractions as well as hydrophobic interactions, are empirically quantified. All of these interactions are related to solvent partitioning phenomena because the dissolution of a 'ligand' in a mixed solvent system (such as water/1-octanol) involves the same fundamental processes and atom-atom interactions as biomolecular interactions within or between proteins and ligands. In practice, HINT 'scores' each atom-atom interaction within or between biological molecules with the following equation:

$$b_{ij} = a_i\, S_i\, a_i\, S_i\, T_{ij}\, R_{ij} + r_{ij}, \qquad (1)$$

where b_{ij} is the interaction score between atoms i and j, a is the hydrophobic atom constant, S is the solvent accessible surface area, T_{ij} is a logic function that uses the specific types and character of the atoms involved in the interaction to set the sign of the score, and R_{ij}/r_{ij} are functions of the distance between atoms i and j (i.e., r). Generally the hydropathic-dependent function, R_{ij}, is the simple exponential e^{-r} [19] and r_{ij} is an implementation of the Lennard-Jones potential function. Thus, r_{ij} is mostly a penalty function to identify and flag too-close atom-atom contacts. The double sum, $\Sigma\Sigma b_{ij}$, is the total interaction score for the system. In HINT favorable interactions are scored with $b_{ij} > 0$ and unfavorable interactions are scored with $b_{ij} < 0$. The logic function T_{ij} returns a value of 1 or -1 depending on the character of the interacting polar atoms (i.e., $a < 0$): there are three possibilities: acid-acid, acid-base, or base-base; only acid-base is scored favorably (see Table 1). T_{ij} also identifies hydrogen bonds which are, as coded in HINT, a special type of acid-base interactions.

The hydrophobic atom constant is the key parameter in the HINT model. The thermodynamic information from the measurement of hydrophobicity is encoded in this constant for each atom. a is calculated by a method similar to the CLOGP [17] method of Hansch and Leo. HINT uses values from a functional group primitive set that is summed and modified by structure-dependent factors which are related to molecular structure [20] and are determined by the connectivity relationships between the group fragments. HINT then calculates the hydrophobic atom constants from the fragment constants *after* these factors have been applied. In general, exposed or frontier atoms of each fragment are assigned $\mathbf{a}_i$ values consistent with their atomistic behavior; e.g., the –OH of a carboxylic acid is assigned the a_i value of an alcoholic –OH. The a_i of other fragment atoms are then adjusted to maintain $\Sigma\ a_i = f_n$. In terms of the HINT calculation of interaction scores, the product $a_i\ S_i$ represents interaction propensity most precisely by including the size and accessibility factor S_i in addition to the atomic (hydropathic) property parameter a_i. Finally, it is significant to note that many other methods of estimating $\mathrm{Log\,P_{o/w}}$ utilize atom-level constants directly, and the potentially significant inter-fragment and intramolecular factors of the CLOGP methodology are never incorporated in the models. Some of these factors, e.g., the polar proximity effect, are second or third order effects that can never be simulated by methods that sum only atom-level constants.

Properties of the HINT model

It is actually an important feature of HINT that all interaction features, i.e., hydrogen bonding, electrostatic and hydrophobic interactions are analyzed and scored with the same mathematical protocol. Differences in HINT scores for different atom-atom interactions are a consequence of the differences in atom properties and the distance between the interacting atoms. Conversely, describing and defining the interactions with different functions, as in molecular mechanics, is really a mathematical construct to simplify discussion of interaction. In nature interactions are concerted; they do not arise from unique 'functions' for hydrogen bonding, Coulombic attraction/repulsion, or hydrophobic attractions. Instead, interactions arise from

Table 1. T_{ij} interaction matrix

Atom Type [atom constant]	*H (apolar)* [a > 0]	*H (polar)*[1] [a > 0]	*C (apolar)* [a > 0]	*Polar (N,O,etc.)* [a < 0]
H (apolar) [a > 0]	+1	-1	+1	+1
H (polar)[1] [a > 0]	-1	-1	-1	-1
C (apolar) [a > 0]	+1	-1	+1	+1
Polar (N,O,etc.) [a < 0]	+1	-1	+1	-1

Notes: green: hydrophobic-hydrophobic; red: hydrophobic-polar; blue: acid-base or hydrogen bond; yellow: polar-polar (horizontal stripes: acid-acid, vertical stripes: base-base).
[1]By convention, all hydrogen atoms have a > 0 [13].

the electronic properties of the atoms. Thus, by design, these core components of a HINT calculation are on a common basis for internal comparison. One of the topics we discuss in this section is that each atom-atom interaction, b_{ij}, is related to a partial δG such that $\Sigma\delta G = \Delta G_{\text{interaction}}$. This is fundamentally different than in molecular mechanics and related approaches where terms from different types of interactions (e.g., electrostatic, hydrophobic, solvation, etc.) are summed to achieve $\Delta G_{\text{interaction}}$. Dill has noted that the universal assumption of additivity for different types of terms may not be valid [21]. Another related topic of this section is the description of an empirical HINT-based method for estimation of desolvation energy in biomolecular associations. However, we will first describe the hydrophobic effect and how it is represented and modeled by HINT.

The hydrophobic effect and the shake-flask

It continues to be a point of argument whether there actually is a 'hydrophobic interaction'. Certainly the major driving force for biological structure is related to the formation of hydrogen bonds, including the development of a structured hydrogen bonding network incorporating water molecules. Thus, small molecules or biomolecular substructures which do not support this 'structure' are pushed aside and tend to congregate themselves. So, does this collection of hydrophobic entities comprise an interaction other than the van der Waals attraction between atoms? The answer is clearly 'no' if entropy is *not* accounted for. However, entropy *is* a significant term for biomolecular associations. Most importantly for our purposes, entropy can arise from the loss or gain in 'structure' of the water network. For example, when a ligand binds to a biomacromolecule, the structured water surrounding the ligand is displaced to bulk (i.e., disordered) solvent, thereby increasing entropy. This is the case even if substantial portions of the ligand are hydrophobic because the waters may still form a network, encasing and isolating the hydrophobe from the bulk solvent. Thus, an additional driving force for biological structure is the gain in entropy from 'released' water molecules, and this is manifested strongly in hydrophobic-hydrophobic interactions. The hydrophobic effect is a combination enthalpic/entropic phenomenon (i.e., it is a free energy phenomenon) [8]. Theoretical analyses by Tanford [5], Nemethy and Scheraga [22] and Ben-Naim [23] reveal much, but fall short of presenting a complete understanding of the hydrophobic effect. It is for these reasons that we believe that understanding and modeling hydrophobicity and hydrophobic 'interactions' is key for understanding biological structure [15].

The simple shake-flask, which is the most basic way to measure hydrophobicity for small molecules, contains two model biological environments. The water layer is like a polar pocket in a biomacromolecule as it has a large number of both hydrogen bond donors and hydrogen bond acceptors. A small molecule that is soluble in this phase must have complementary hydrogen bond donors and/or acceptors. The 1-octanol layer

is similar to a hydrophobic pocket or cleft in a biomacromolecule. It is capable of forming hydrophobic-hydrophobic interactions with appropriate functional groups on small molecules that are soluble in this phase (or perhaps *in*soluble in the water phase). There may be some ordering of the alcohol head groups at the water/1-octanol interface; the choice, in part, of 1-octanol as the 'standard' lipophilic solvent was based on a chemical and structural analogy of 1-octanol to lipids in bilayer membranes. Interestingly, water itself has a measurable $\mathrm{Log\,P_{o/w}}$, -1.38, and there is evidence that some molecules 'drag' water [24] into the 1-octanol layer. This particular two-solvent system is complex! However, this complexity adds to the value of $\mathrm{Log\,P_{o/w}}$, making it a more realistic 'model' for hydrophobic regions of biomacromolecules than aliphatic or aromatic hydrocarbon solvents.

The hydrophobic constant, a_i, for an atom encodes the preference of that atom for one of the two solvents. In 'interacting' two atoms, the sign of the product $a_i\ a_j$ determines whether the interaction is compatible ($a_i\ a_j > 0$) on a hydropathic basis. In HINT, hydrogen bonds and other polar-polar interactions are sorted out with atomic descriptor variables (*vide supra*). From the perspective of the shake-flask $a_i\ a_j > 0$ represents 'solubility' in one of the two phases, while $a_i\ a_j < 0$ represents 'insolubility', i.e., a hydrophobic-polar interaction. These hydrophobic-polar interactions are related to the energy of desolvation, which will be discussed below.

Free energy of interaction

The shake-flask experiment, or any other means of measuring $\mathrm{Log\,P_{o/w}}$, is fundamentally a free energy experiment. In fact, this is a rare *direct* measurement of interaction. $\mathrm{Log\,P_{o/w}}$ and also hydrophobic fragment and atom constants are *free-energy-like* thermodynamic parameters. $P_{o/w}$ is the equilibrium constant for solute transfer between the 1-octanol and water solvents such that

$$\mathrm{Log_{10}\,P_{o/w}} = \Delta G\ /\ 2.303RT, \tag{2}$$

where RT is generally a constant. This can be rewritten as

$$\mathrm{Log\,P_{o/w}} = \Delta G\ /\ k, \tag{3}$$

($k = -1.364$ kcal mol^{-1} at 298 K). The summation of all a_i for a molecule is $\mathrm{Log\,P_{o/w}}$; therefore $a_i \approx \delta G$. Note that the a are *dimensionless* parameters directly related to the free energy of atom transfer. Because $a_i\ a_j\ k$ has energy units of kcal mol^{-1}, it is readily apparent that the HINT score b_{ij} represents a free energy-like term. However, in our development of HINT we have found it necessary to calibrate the calculational model for each molecular system, i.e., we have to empirically determine a factor relating $\Sigma\ \Sigma\ b_{ij}$ to experimental free energy of association (binding) for each system [14]. This is likely due to a variety of factors mostly associated with the quality of the macromolecule crystallographic structures. A key, but less obvious, factor among these is the contribution of structurally-conserved water molecules. The quantity of 'observed' and reported water molecules in X-ray crystallographic structures correlates very significantly with the resolution of the crystallographic experiments. Accurate thermodynamic predictions appear to require inclusion of these water molecules as part of the model [16].

The system we have studied in most detail is hemoglobin. There are two structurally distinct endpoints of the hemoglobin allosteric transition, representing full oxygenation of the four subunits (termed *oxy* or Relaxed (R) state) and full deoxygenation (termed *deoxy* or Tense (T) state). Both endpoints [25, 26] have been crystallographically characterized as have a number of site-specific mutations [27]. In addition, solution thermodynamic measurements of the free energies of dimer-tetramer assembly for dozens of mutant hemoglobins are available [28]. Pairs of the four hemoglobin subunits ($\alpha_1\beta_1$ and $\alpha_2\beta_2$) are termed dimers. These dimers maintain their structural integrity, while changing contacts with respect to each other, as hemoglobin undergoes allosteric transitions due to changing oxygenation. Thus, the intradimer contacts, i.e., between α_1 and β_1 and between α_2 and β_2, change little. In contrast, the interdimer contacts, i.e., between α_1 and α_2, between α_1 and β_2, between α_2 and β_1 and between β_1 and β_2, are significantly different in *oxy* and *deoxy* hemoglobin. In fact, β_1-β_2 contacts only exist in *oxy* hemoglobin. To calibrate HINT for hemoglobin we summed the $\Sigma\Sigma b_{ij}$ for this latter set of interdimer subunit-subunit contacts in *deoxy* hemoglobin, and divided this number by the measured $\Delta G_{\mathrm{dimer}\rightarrow\mathrm{tetramer}}$ for normal *deoxy* hemoglobin to determine the calibration factor of -515 HINT units per kcal mol^{-1} [14, 16]. This factor proved to be useful for analyzing both *oxy* and *deoxy* variants of a large variety of site-specific mutants that have widely ranging allosteric and thermodynamic properties [29].

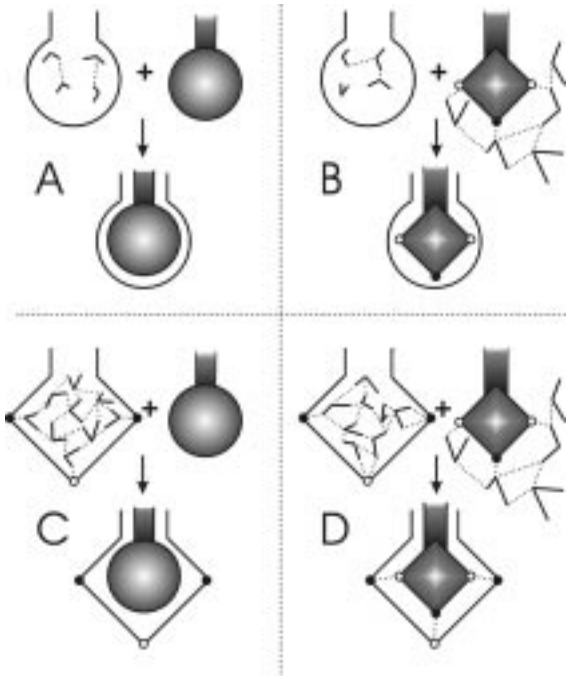

Figure 1. Examples of Polar and Hydrophobic Interactions. Curved surfaces represent hydrophobic entities, vertices are polar groups where open circles are hydrogen bond acceptors and closed circles are hydrogen bond donors. A) A hydrophobic pocket accepting a hydrophobic fragment. Note the water molecules in the pocket are associated with each other but not with the biomacromolecule. If these are displaced to bulk, there will be an increase in entropy. B) A hydrophobic pocket accepting a polar fragment. The fragment is 'desolvated' by this event. C) A polar pocket accepting a hydrophobic fragment. Pocket is desolvated. D) A polar pocket accepting a polar fragment. A lot of water is displaced to bulk, but energetically both the fragment and the macromolecule maintain similar favorable interactions.

Modeling water molecules as small independent ligands

As mentioned above one of the key factors for accurately modeling free energy of association is including the interactions tendered by structurally conserved water molecules. Our approach is to treat the water molecules as small independent ligands that are individually bound as part of the biomolecular system. Their interactions with the biomolecules are examined and tabulated as a component of $\Delta G_{\text{interaction}}$, e.g., $\Delta G_{\text{interaction}} = \Delta G_{\text{A-B}} + \Delta G_{\text{AB-W}}$, where $\Delta G_{\text{A-B}}$ is the association between biomolecules A and B and $\Delta G_{\text{AB-W}}$ is the association between the AB complex and waters. In this model the internal water-water contacts are ignored. They are presumed to be, in part, modeled by the entropic component of the HINT hydrophobic atom constants.

We have found that applying the GRID program of Goodford [30] with a water probe partially circumvents the issues of variable quality and availability of crystallographic water coordinates. In addition, this approach allows modeling of biomacromolecular structures, e.g., complexes or mutants, for which experimental structural data does not yet exist [29]. We have also developed an automated procedure for optimizing orientation and position of individual watermolecules using the HINT score paradigm (Equation 1) (unpublished data). Because the criteria for ideal interactions are different between the HINT 'force field' and molecular mechanics force fields, this procedure does yield somewhat different 3D structures for the water molecules in biomacromolecular complexes. We are investigating and validating this algorithm on several series of protein-protein and protein-ligand complexes, and present an example below.

Energy of desolvation

Electrostatic potential codes using the Poisson–Boltzmann algorithm have been used to calculate solvation energy for small molecules or biomacromolecules [31]. These approximations are based on the relative dielectric constants 'inside' and 'outside' the molecule, where 'outside' refers to water, i.e., $\varepsilon = 80$. The 'inside' dielectric is generally assumed to be a constant around 2–5. While this approach simulates the "stripping" of water as a ligand binds to a uniform low-dielectric environment, it does not take into account the types of interactions that the ligand's individual functional groups engage in when bound (See Figure 1). For example, a polar functional group located in a polar pocket (Figure 1D) would not incur as significant a desolvation energy cost as the same functional group in a hydrophobic pocket (Figure 1B). Likewise there is a desolvation energy cost with respect to water (solvent) associated with polar portions of the receptor being displaced by the incoming ligand. If the ligand fragment is hydrophobic (Figure 1C) this could be significant.

The HINT algorithm is ideal for quantifying the 'matches' of polar and hydrophobic molecular fragments. There are three types of interactions: polar-polar, hydrophobic-hydrophobic and hydrophobic-polar. The polar-polar interactions can be either favorable or unfavorable depending on charge and acid-base character as described above, and the hydrophobic-hydrophobic interactions are always favorable. In

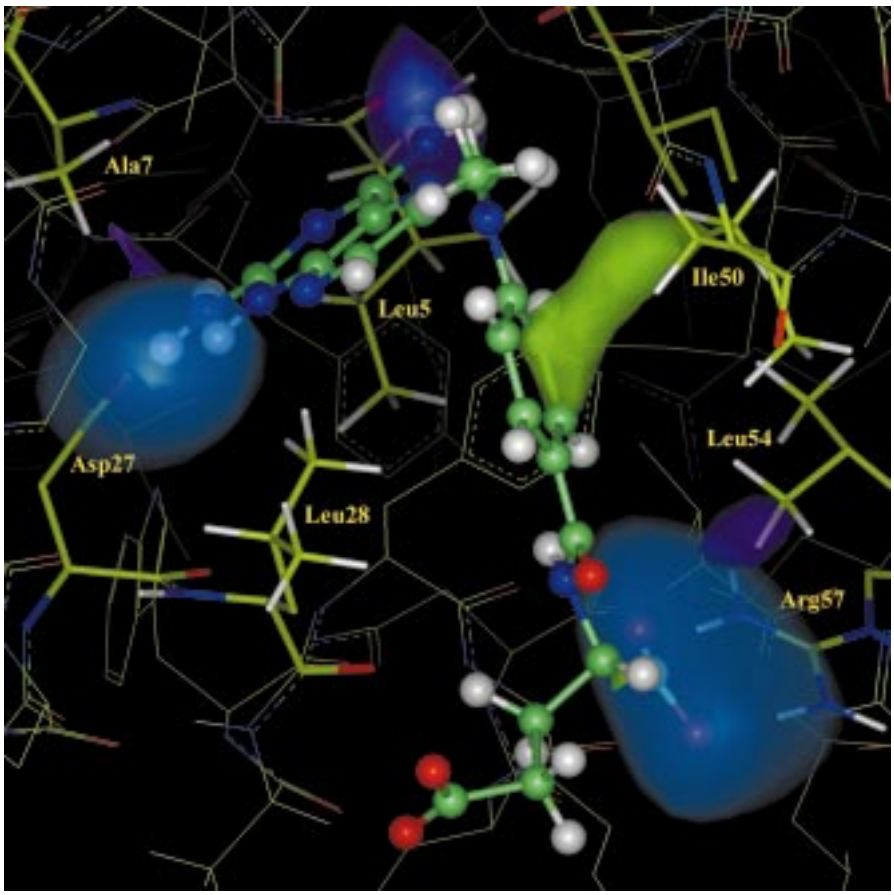

Figure 2. HINT map of interactions between methotrexate (MTX) and dihydrofolate reductase (DHFR). MTX is displayed in ball and stick, important DHFR residues are displayed with stick and labeled, while the remainder of DHFR is displayed as lines. The 3D contours are spatial representations of the type (color) and strength (contour volume) of the interactions between the interacting molecules. Blue contours represent favorable acid-base interactions and are most often correlated with hydrogen bonds. The green contours represent hydrophobic-hydrophobic interactions. The purple contours represent hydrophobic-polar interactions. Contour levels are as follows: +50 for acid-base/hydrogen bond, −50 for hydrophobic-polar and +20 for hydrophobic-hydrophobic.

terms of desolvation, polar-polar interactions represent cases where (unbound) water-associated fragments are translated to a similar (polar) environment when bound. There is no reason to believe that this is a totally neutral event, energy-wise, but in keeping with the premise of HINT, it is not an unreasonable approximation to consider it so.

However, more significant is that hydrophobic-polar interactions are scored by HINT as unfavorable and therefore contribute 'negatively' to the energetics of binding, i.e., $\Delta G > 0$. What do HINT hydrophobic-polar interactions represent? They are the 'forced' association of hydrophobic atoms or fragments with polar atoms or fragments. This is precisely what is happening in ligand/biomacromolecule desolvation. Therefore the HINT hydrophobic-polar interaction score term is an empirical free-energy estimate for the energy cost to desolvate the polar portions of the ligand or 'receptor' by placing them in a hydrophobic environment. It is interesting to note that hydrophobic-polar interaction scores are generally the largest source of unfavorable interactions in HINT studies which suggests that desolvation is a critical factor in free energy of ligand binding.

An example HINT analysis: methotrexate/dihydrofolate reductase

To illustrate the points made in the previous section we have analyzed the well-known dihydrofolate reductase (DHFR) / methotrexate (MTX, **I**) complex with HINT.

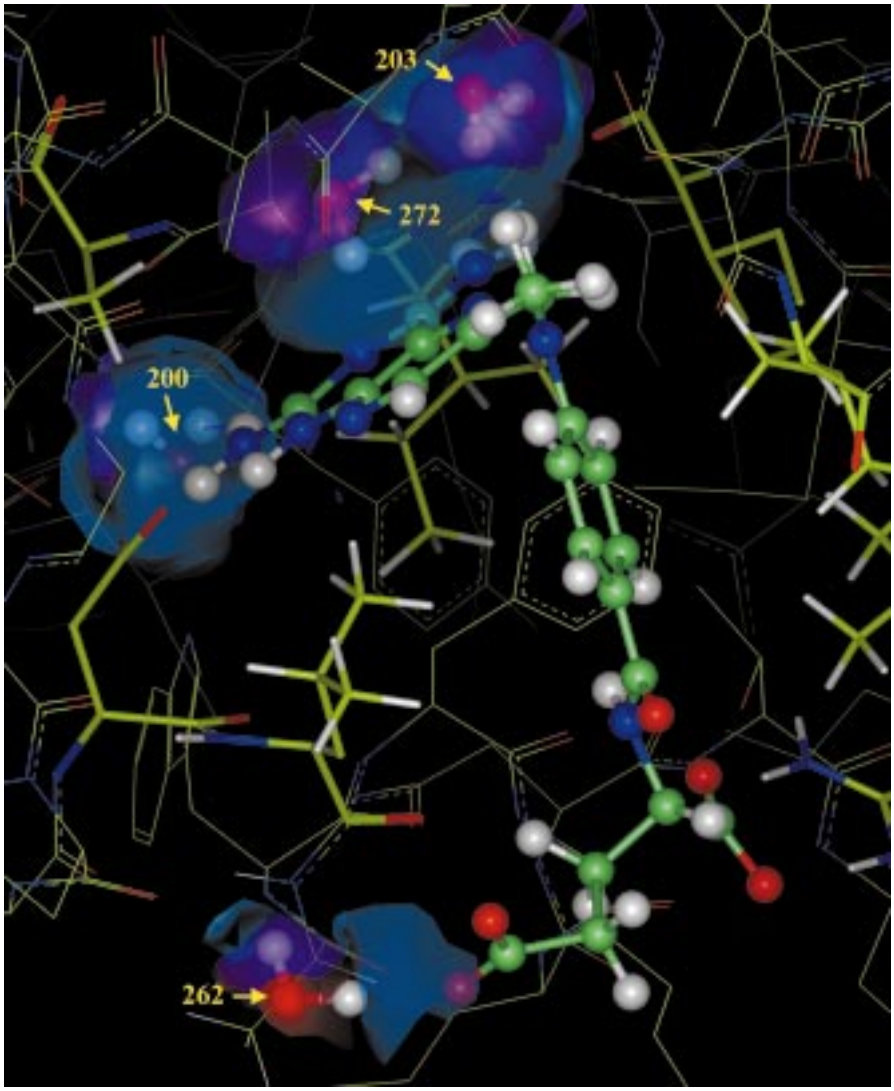

Figure 3. HINT map of summed interactions between methotrexate and water set (described in text) and dihydrofolate reductase and water set. Water molecules are labeled with their PDB HETATM record numbers. Blue contours (level +75) represent favorable acid-base interactions and are most often correlated with hydrogen bonds. The red contours (level −75) represent unfavorable polar-polar interactions. The purple contours (level −75) represent hydrophobic-polar interactions. There are no hydrophobic-hydrophobic interactions.

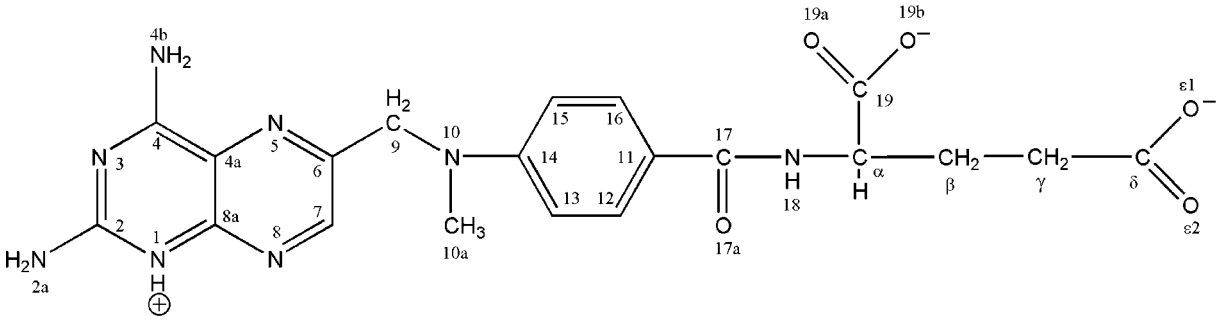

Scheme . Methotrexate (MTX).

Methotrexate is a potent inhibitor of the oxidoreductase enzyme with a nearly irreversible $K_i \leq 0.1$ nM [32]. The following study is a brief analysis of only one, albeit one of the most potent, of the known inhibitors of DHFR. An exhaustive analysis of the entire previously reported series of MTX derivatives [33] is beyond the scope or intent of the present report.

Methodology

The X-ray structure of *E. coli* dihydrofolate reductase complexed with methotrexate was taken from the Protein Data Bank as entry 1RG7 [34]. This structure has a resolution of 2.0 Å. Using insightII [35] hydrogens were modeled to the structure at pH 7.0 and the N1 position of MTX was protonated as in **I** above. The hydrogens in the resulting structure were minimized for 100 cycles to remove bad contacts. At this point the structure was resolved into three components: enzyme, drug and water. Four of the crystallographically determined water molecules, 200, 203, 262 and 272, were found to have significant interactions with *both* DHFR and MTX. These were designated as the water set for this study. To verify that these water molecules are accurately placed and significant, the GRID program using the H_2O probe [30] was employed over the MTX binding region. All four of these water molecules were found to corresponded to favorable GRID energy contours. Three HINT score calculations were performed: between MTX and DHFR (see Table 2), between MTX and the water set, and between DHFR and the water set. Initially the water set gave unfavorable HINT scores: MTX/water (703) and DHFR/water (−1111); total (−408). Thus, the HINT ligand optimization function was used to optimize the 4 interfacing waters. In the first step, each water was minimized to a convergence of 0.01 HINT score units and allowed to move within a 0.5 Å sphere. Two of the four waters still produced negative total HINT scores and were subjected to a second HINT ligand optimization. The four water molecules moved an average of 0.66 Å from their original positions, but had significantly more favorable HINT interaction scores: MTX/water (1579) and DHFR/water (−987); total (566) (See also Table 3).

Results

A list of significant HINT score interactions between DHFR and MTX is set out in Table 2. This list indicates that there are 10 hydrogen bonds between the enzyme and inhibitor, with HINT scores ranging between 136 and 789. HINT scores hydrogen bonds similarly to acid-base interactions except that a hydrogen bond must involve both a hydrogen bond donor and an acceptor and have a specific distance cutoff, which is 3.65 Å in this study. It is clear that the higher-scoring hydrogen bonds are of the ionic-reinforced type, e.g., between carboxylate oxygens (O19a and O19b) of MTX and arginine (ARG 57) nitrogens of DHFR. There are also two special hydrogen bonds, between polar hydrogen bond donors NH1 and NH2 and the unsaturated MTX carbon C19. This type of interaction has been described previously in biological structure [36, 37]. There are a large number of other acid-base interactions, many of which are not enumerated in Table 2, that contribute to the binding. In addition, a substantial number of favorable hydrophobic-hydrophobic interactions, e.g., surrounding the aromatic ring and methyl carbon of MTX, round out the favorable interactions.

Two sources of unfavorable ($b_{ij} < 0$) interactions are seen in the MTX/DHFR association. First, what we refer to as base-base interactions, e.g., between ring nitrogen N8 of MTX and Asp 27 carboxylate oxygens, can be alternatively considered as Coulombic repulsions. In many cases these can be remediated with bridging water molecules. In other cases protonation of a carboxylate to form a carboxylic acid functional group is appropriate. The second type of unfavorable interactions involve hydrophobic-polar contacts that occur when a polar functional group and a hydrophobic functional group interact. Succinct examples of this in Table 2 are interactions between the side-chain methyls of Leu 54 and the MTX carboxylate oxygens O19a and O19b. There is a general inevitable background of this type of hydrophobic-polar interaction in any biomacromolecular system. For drug design purposes, one would want to ameliorate as many of these unfavorable interactions as is possible to achieve tighter binding.

HINT also calculates a contourable 3D interaction map that visually displays the type (by color) and relative intensity (by contour volume) of interactions between two molecules. The details of performing this calculation have been presented elsewhere [11]. Such a map is presented as Figure 2 for the association of methotrexate with dihydrofolate reductase. The features of this map can be correlated with the numerical results of Table 2 to gain both a qualitative and quantitative 3D understanding of the binding event. Qualitatively, at the chosen contour levels, there are four

Table 2. HINT Interactions between Methotrexate and Dihydrofolate reductase[a].

Methotrexate		Dyhydrofolate reductase				Interaction		
Atom	a_i	Residue		Atom	a_j	r (Å)	Score	Class
N1	−0.354	ALA	7	CB	0.810	3.96	−62	Hydrophobic-Polar
N1	−0.354	ALA	19	CB	0.810	3.94	−55	Hydrophobic-Polar
N1	−0.354	ASP	27	OD1	−3.310	3.55	145	Hydrogen Bond
N1	−0.354	ASP	27	OD2	−3.310	2.73	489	Hydrogen Bond
C2	0.890	ALA	7	CB	0.810	3.92	31	Hydrophobic
C2	0.890	ASP	27	OD1	−3.310	3.77	70	Acid-Base
C2	0.890	ASP	27	OD2	−3.310	3.63	81	Acid-Base
N2a	−0.276	ILE	5	CD1	0.820	4.70	−60	Hydrophobic-Polar
N2a	−0.276	ALA	7	CB	0.810	3.77	−135	Hydrophobic-Polar
N2a	−0.276	ASP	27	OD1	−3.310	2.81	452	Hydrogen Bond
N2a	−0.276	ASP	27	OD2	−3.310	3.41	187	Hydrogen Bond
N4b	−0.244	ILE	5	O	−1.915	2.79	180	Hydrogen Bond
N4b	−0.244	ILE	5	CG2	0.820	3.91	−100	Hydrophobic-Polar
N4b	−0.244	ALA	6	CB	0.810	4.89	−53	Hydrophobic-Polar
N4b	−0.244	ILE	94	O	−1.915	3.00	136	Hydrogen Bond
C7	0.355	ALA	19	CB	0.810	3.46	31	Hydrophobic
C7	0.355	LEU	28	CD2	0.820	3.64	24	Hydrophobic
N8	−0.923	ALA	19	CB	0.810	3.24	−61	Hydrophobic-Polar
N8	−0.923	ASP	27	OD2	−3.310	3.62	−80	Base-Base
C8a	1.237	ALA	7	CB	0.810	4.59	22	Hydrophobic
C8a	1.237	ALA	19	CB	0.810	3.46	65	Hydrophobic
C8a	1.237	ASP	27	OD2	−3.310	3.56	116	Acid-Base
C8a	1.237	LEU	28	CD2	0.820	4.43	22	Hydrophobic
C9	0.492	THR	46	CG2	0.810	3.89	30	Hydrophobic
C9	0.492	ILE	50	CD1	0.820	4.36	21	Hydrophobic
C10a	0.806	ALA	18	O	−1.915	3.56	−73	Hydrophobic-Polar
C10a	0.806	ASN	23	OD1	−1.915	4.22	−50	Hydrophobic-Polar
C10a	0.806	THR	46	CG2	0.810	4.93	22	Hydrophobic
C10a	0.806	SER	49	CB	0.489	3.65	36	Hydrophobic
C10a	0.806	ILE	50	CD1	0.820	4.84	26	Hydrophobic
C15	0.355	ILE	50	CD1	0.820	3.70	23	Hydrophobic
C17	1.045	LEU	54	CD2	0.820	3.99	30	Hydrophobic
O17a	−1.915	ARG	52	NH2	−1.540	4.44	63	Acid-Base
O17a	−1.915	LEU	54	CD2	0.820	4.35	−51	Hydrophobic-Polar
N18	−0.623	LEU	54	CD2	0.820	3.88	−51	Hydrophobic-Polar
C19	3.444	LYS	32	CB	0.477	3.88	24	Hydrophobic
C19	3.444	LEU	54	CD1	0.820	5.37	22	Hydrophobic
C19	3.444	LEU	54	CD2	0.820	3.78	107	Hydrophobic
C19	3.444	ARG	57	NH1	−1.540	3.39	187	Hydrogen Bond*
C19	3.444	ARG	57	NH2	−1.540	3.42	172	Hydrogen Bond*
O19a	−3.310	LEU	28	O	−1.915	4.64	−59	Base-Base
O19a	−3.310	PHE	31	CE2	0.355	3.49	62	Acid-Base
O19a	−3.310	LEU	54	CD1	0.820	4.78	−62	Hydrophobic-Polar
O19a	−3.310	LEU	54	CD2	0.820	3.76	−170	Hydrophobic-Polar
O19a	−3.310	ARG	57	NH1	−1.540	2.51	789	Hydrogen Bond

Table 2 continued.

Methotrexate		Dyhydrofolate reductase				Interaction		
Atom	a_i	Residue		Atom	a_j	r (Å)	Score	Class
O19a	−3.310	ARG	57	NH2	−1.540	3.33	250	Hydrogen Bond
O19b	−3.310	LYS	32	NZ	−2.214	4.48	79	Acid-Base
O19b	−3.310	ARG	52	NH2	−1.540	4.27	107	Acid-Base
O19b	−3.310	LEU	54	CD2	0.820	4.22	−108	Hydrophobic-Polar
O19b	−3.310	ARG	57	NH1	−1.540	3.51	222	Hydrogen Bond
O19b	−3.310	ARG	57	NH2	−1.540	2.77	595	Hydrogen Bond
Cδ	2.416	LEU	28	CD1	0.820	4.91	24	Hydrophobic
Oε1	−3.310	LEU	28	CD1	0.820	4.34	−96	Hydrophobic-Polar
Oε2	−3.310	LEU	28	O	−1.915	4.43	−72	Base-Base
Oε2	−3.310	ALA	29	CB	0.810	5.08	−52	Hydrophobic-Polar
Oε2	−3.310	LYS	32	NZ	−2.214	4.71	87	Acid-Base

[a]Interactions are filtered as follows: hydrophobic-hydrophobic interactions with a score less than 20 and polar interactions with |score| less than 50 have been excluded for brevity.

major regions of interaction evident in Figure 2. The blue contours around atoms N1 and N2a and around carboxylate atoms C19, O19a and O19b of MTX indicate the major hydrogen bonding regions between the enzyme and inhibitor. Carbons of the aromatic ring of MTX are involved in a variety of hydrophobic-hydrophobic interactions with ILE 50; this is plotted as the green contour in Figure 2. Lastly, there are a small number of hydrophobic-polar interactions (purple contours) evident in Figure 2. These generally occur in regions that are also supporting very favorable polar interactions, e.g., the interactions between the carboxylate of MTX and ARG 57 in the lower right hand of Figure 2. The small hydrophobic-polar interaction between the carboxylate and LEU 54 is not particularly important, and is almost inevitable considering the spatial proximity of ARG 57 and LEU 54 in the protein.

HINT maps of the MTX/water and DHFR/water interactions were summed and contoured as shown in Figure 3. From this picture the importance of water is evident. The four water molecules are each enveloped in contours representing favorable (blue) and unfavorable (red and purple) interactions. A classic example of a bridging water is 262, which bridges by hydrogen bond donation to both the backbone carbonyl oxygen (O) of PRO 25 and one of the terminal carboxylate oxygens of MTX.

The HINT scores for the three intermolecular interaction sets (DHFR/MTX, MTX/water and DHFR/water) are summarized in Table 3. It is interesting that, even after optimization, the water set makes an overall favorable interaction (score: 1579) with the inhibitor but an overall unfavorable interaction (score: −987) with the enzyme. This may indicate that the inhibitor 'dragged' one or more of the water molecules with it into the binding site.

We choose to think of the binding process of methotrexate with dihydrofolate reductase as something like

$$\mathrm{DHFR} \cdot x\mathrm{H_2O} + \mathrm{MTX} \cdot y\mathrm{H_2O} \rightarrow$$
$$\mathrm{DHFR} \cdot \mathrm{MTX} \cdot 4\mathrm{H_2O} + (x + y - 4)\mathrm{H_2O},$$

where there are unknown numbers of water molecules initially associated with the uncomplexed enzyme (x) and the free inhibitor (y) that are potentially displaced by the binding event. Four of these initial water molecules perform important bridging functions in the complex, while the others (x+y−4) are released to bulk, thereby increasing entropy. We have analyzed in this study only the DHFR·MTX·$4H_2O$ complex. However, as we stated above, it is possible to infer much about the thermodynamics of binding through this single analysis.

The K_i for MTX of $\leq$ 0.1 nM corresponds to $\Delta G \leq -13.6$ kcal mol^{-1}. The total HINT score of 4600, which should correlate with ΔG, suggests that ≈ -340 HINT score units [(4600/13.6)] are equivalent to one kcal mol^{-1}. With this assumption, the hydrogen bonds between MTX and DHFR (Table 2) range in strength from −0.4 to −2.3 kcal mol^{-1}. The hydrophobic-polar 'cost of desolvation' is about +13.9 kcal mol^{-1}, which is about a third of the favorable polar interactions (acid-base and hydrogen bonds) of −38.3 kcal mol^{-1}. Hydrophobic-hydrophobic interactions are only modestly significant in this system,

Table 3. Summary of HINT intermolecular scores between MTX, DHFR, and adjacent significant water molecules

	Hydropathic interactions						
	Hydrogen Bond	Acid-Base	Hydrophobic	Base-Base	Acid-Acid	Hydrophobic-Polar	Total
MTX/DHFR	3597	2259	1677	−764	0	−2761	**4008**
MTX/Water	3195	1075	0	−879	−1666	−146	**1579**
DHFR/Water	1727	1177	0	−538	−1551	−1802	**−987**
Total	**8519**	**4511**	**1677**	**−2181**	**−3217**	**−4709**	**4600**

contributing −4.9 kcal mol^{-1}. Finally, the combination of unfavorable acid-acid and base-base interactions, which mostly arise from the interactions involving water, is +15.9 kcal mol^{-1}. On average, each water molecule stabilizes the system by −0.4 kcal mol^{-1}, which is similar to previous observations in HINT analyses [14, 16] and other methods [38].

Conclusions

There are a large number of force field methods utilizing molecular mechanics equations to optimize structures and interactions that have been enormously successful in describing biomacromolecular structure. This approach, however, is often limited by its use of an incomplete thermodynamic cycle. These methods are targeted upon calculation of enthalpy and have limited means to calculate or estimate entropy and desolvation. By utilizing a *very empirical* source of *interaction* data, the partition coefficient for 1-octanol/water solubility, Log $P_{o/w}$, we have been developing the empirical HINT force field for non-covalent interactions. This new force field is designed to be a *free energy* force field. There are many approximations in the HINT model and calculations arising from a variety of sources, including errors and omissions in hydrophobicity data bases, simplistic approaches to estimating hydrophobic and solvent accessible surface area atom constants, and errors in macromolecular crystallography. Notwithstanding, calculations on a number of biomolecular systems have shown useful correlation between HINT score and $\Delta G_{\text{interaction}}$. We are continuing to characterize and expand the capabilities of the HINT model.

Acknowledgements

We gratefully acknowledge the support of the National Institutes of Health (grant 5R01HL32793-15 to D.J.A.) and Virginia Commonwealth University. Tripos, Inc. (www.tripos.com), and Molecular Simulations, Inc. (www.msi.com) have provided software to V.C.U. for teaching and research. eduSoft, LC (www.edusoft-lc.com) partially supports the development of HINT.

References

1. a. Petukhov, M., Cregut, D., Soares, C.M. and Serrano, L., Protein Sci., 8 (1999) 1982.
b. Royer, W.E., Jr., Pardanani, A., Gibson, Q.H., Peterson, E.S. and Friedman, J.M., Proc. Natl. Acad. Sci. USA, 93 (1996) 14526.
c. Bhat, T.N., Bentley, G.A., Boulot, G., Greene, M.I., Tello, D., Dall'Acqua, W., Souchon, S., Schwarz, F.P., Mariuzza, R.A. and Poljak, R.J., Proc. Natl. Acad. Sci. USA, 91 (1994) 1089.
2. Berman, H.M, Westbrook, J., Feng, Z., Gilliland, G., Bhat, T.N., Weissig, H., Shindyalov, I.N. and Bourne, P.E., Nucl. Acids Res., 28 (2000) 235.
3. a. Dixon, R.W. and Kollman, P.A., Proteins Struct. Funct. Genet., 36 (1999) 471.
b. Cornell, W.D., Cieplak, P. and Bayly, CI., J. Am. Chem. Soc., 117 (1995) 5179.
c. Jones-Hertzog, D.K. and Jorgensen, W.L., J. Med. Chem., 40 (1997) 1539.
d. Aqvist, J., Medina, C. and Samuelsson, J.E., Protein Eng., 7 (1994) 385.
e. Reddy, M.R., Varney, M.D., Kalish, V., Viswanadhan, V.N. and Appelt, K., J. Med. Chem., 37 (1994) 1145. f. Rao, B.G., Tilton, R.F. and Singh, U.C., J. Am. Chem. Soc., 114 (1992) 4447.
g. Massova, I. and Kollman, P.A., J. Am. Chem. Soc., 121 (1999) 8133. h. Gao, J., Kuczera, K., Tidor, B. and Karplus, M., Science, 244 (1989) 1069. h. Vallone, B., Miele, A.E., Vecchini, P., Chiancone, E. and Brunori, M., Proc. Natl. Acad. Sci., USA 95 (1998) 6103.
i. Zeng, J., Fridman, M., Maruta, H., Treutlein, H.R. and Simonson, T., Protein Sci., 8 (1999) 50. j. Venkatarangan, P. and Hopfinger, A.J., J. Med. Chem., 42 (1999) 2169.
k. Pearlman, D.A. and Connelly, P.R., J. Mol. Biol., 248 (1995) 696.
l. Tawa, G.J., Topol, I.A., Burt, S.K. and Erickson, J.W., J. Am. Chem. Soc., 120 (1998) 8856.
4. Kellogg, G.E., Med. Chem. Res., 9 (1999) 439.

5. Tanford, C., The Hydrophobic Effect: Formation of Micelles and Biological Membranes, 2nd edition, Wiley, New York, NY, 1980.
6. a. Lum, K., Chandler, D. and Weeks, J.D., J. Phys. Chem. 103 (1999) 4570.
   b. Tsai, C.J. and Nussinov, R., Prot. Sci., 6 (1997) 24.
   c. Roseman, M.A., J. Mol. Biol., 200 (1988) 513.
   d. Eisenberg, D., Wilcox, W. and McLachlan, A.D., J. Cell Biochem., 31 (1986) 11. e. Eisenberg, D. and McLachlan, A.D., Nature, 319 (1986) 199.
7. a. White, S.H. and Jacobs, R.E., J. Membrane Biol., 115 (1990) 145. b. Westkaemper, R.B. and Glennon, R.A., Med. Chem. Res., 3 (1993) 317.
8. Hansch, C., Leo, A., Exploring QSAR. Fundamentals and Applications in Chemistry and Biology, American Chemical Society, Washington, 1995.
9. Hansch, C., Steward, A.R., Anderson, S.M. and Bentley, D. , J. Med. Chem., 11 (1968) 1.
10. a. Mannhold, R. and Rekker, R.F., Persp. Drug Discov. Design, 18 (2000) 1.
    b. Mannhold, R. and Dross, K., Quant. Struct. Act. Relat., 15 (1996) 403.
    c. Leo, A.J., Chem. Rev., 93 (1993) 1281.
11. Wireko, F.C., Kellogg, G.E. and Abraham, D.J., J. Med. Chem., 34 (1991) 758.
12. Kellogg, G.E., Semus, S.F. and Abraham, D.J., J. Comput. Aided Mol. Des., 5 (1991) 545.
13. Kellogg, G.E., Joshi, G.S. and Abraham, D.J., Med. Chem. Res., 1 (1992) 444.
14. Abraham, D.J., Kellogg, G.E., Holt, J.M. and Ackers, G.K., J. Mol. Biol., 272 (1997) 613.
15. Kellogg, G.E. and Abraham, D.J., Eur. J. Med. Chem., 35 (2000), 651.
16. Burnett, J.C., Kellogg, G.E. and Abraham, D.J., Biochem. 39 (2000) 1622.
17. Hansch, C. and Leo, A.J., Substituent Constants for Correlation Analysis in Chemistry and Biology, Wiley, New York, NY, 1979.
18. Kyte, J. and Doolittle, R.F., J. Mol. Biol., 57 (1982) 105.
19. Isrealachvili, J. and Pashley, R., Nature, 300 (1982) 341.
20. a. Abraham, D.J. and Leo, A.J., Proteins, 2 (1987) 130.
    b. Abraham, D.J. and Kellogg, G.E., J. Comput. Aided Mol. Des., 8 (1994) 41.
21. Dill, K.A., J. Biol. Chem., 272 (1997) 701.
22. a. Nemethy, G. and Scheraga, H., J. Chem. Phys., 36 (1962) 3382.
    b. Nemethy, G. and Scheraga, H., J. Phys. Chem., 66 (1962) 1773.
23. Ben-Naim A., Hydrophobic Interactions, Plenum, New York, NY, 1980.
24. a. Tsai, R.S., Fan, W.Z., ElTayar, N., Carrupt, P.A., Testa, B. and Kier, L., J. Am. Chem. Soc., 115 (1993) 9632.
    b. Fan, W.Z., Tsai, R.S., ElTayar, N., Carrupt, P.A. and Testa, B., J. Phys. Chem., 98 (1994) 329.
25. Fermi, G., Perutz, M.F., Shaanan, B. and Fourme R., J. Mol. Biol., 175 (1984) 159.
26. Shaanan, B., J. Mol. Biol., 171 (1983) 31.
27. a. Smith, F.R., Lattman, E.E. and Carter, C.W., Jr., Proteins: Struct. Funct. Genet., 10 (1991) 81.
    b. Kavanaugh, J.S., Weydert, J.S. and Ackers, G. K., Biochemistry, 37 (1998) 4358.
    c. Kavanaugh, J.S., Rogers, P.H., Case, D.A. and Arnone, A., Biochemistry, 31 (1992) 4111.
    d. Harrington, D.J., Adachi, K. and Royer, W.E., Jr., J. Biol. Chem., 273 (1998) 32690.
    e. Ishimori, K., Morishima, I., Imai, K., Fushitani, K., Miyazaki, G., Shih, D., Tame, J., Pegnier, J. and Nigai, K., J. Biol. Chem., 264 (1989) 14624.
    f. Kavanaugh, J.S., Chafin, D.R., Arnone, A., Mozzarelli, A., Rivetti, C., Rossi, G.L., Kwiatkowski, L.D. and Noble, R.W., J. Mol. Biol., 248 (1995) 136.
    g. Silva, M.M., Rogers, P.H. and Arnone, A., J. Biol. Chem., 267 (1992) 17248.
28. a. Turner, G.J., Galacteros, F., Doyle, M.L., Hedlund, B., Pettigrew, D.W., Turner, B.W., Smithm F.R., Moo-Pen, W., Rucknagel, D.L. and Ackers, G.K., Proteins: Struct. Funct. Genet., 14 (1992) 333.
    b. LiCata, V.J., Dalessio, P.M. and Ackers, G.K., Proteins: Struct. Funct. Genet., 17 (1993) 279.
    c. Kiger, L., Klinger, A.L., Kwiatkowski, L.D., Young, A.D., Doyle, M.L., Holt, J.M., Noble, R.W. and Ackers, G.K., Biochemistry, 37 (1988) 4336.
29. Burnett, J.C., Botti, P., Abraham, D.J. and Kellogg, G.E., Proteins Struct. Funct. Genet. Proteins: Struct. Fund. Genet., 42 (2001) 355–377.
30. Goodford, P.J., J. Med. Chem., 28 (1985) 857.
31. Gilson, M.K. and Honig, B., Proteins: Struct. Funct. Genet., 4 (1988) 7.
32. a. Burchall, J.J., in Hitchings, G.H. (Ed.), Inhibition of Folate Metabolism in Chemotherapy. The Origins and Uses of Cotrimoxazole, Springer-Verlag, Berlin, 1983, pp. 55–74.
    b. Burchall, J.J., in Sirotnak, F.M., Burchall, J.J., Ensminger, W.B. and Montgomery, J.A. (Eds), Folate Antagonists as Therapeutic Agents 1. Biochemistry, MolecularActions, and Synthetic Design, Academic, Orlando, 1984, pp. 133–150.
33. Montgomery, J.A. and Piper, J.R., in reference 32b, pp. 219–260.
34. Sawaya, M.R. and Kraut, J. Biochemistry, 36 (1997) 586.
35. Molecular Simulations, Inc., San Diego CA.
36. Levitt, M. and Perutz, M.F., J. Mol. Biol., 201 (1988) 751.
37. a. Perutz, M.F., Fermi, G., Abraham, D.J., Poyart, C. and Bursaux, E., J. Am. Chem. Soc., 108 (1986) 1064.
    b. Burley, S.K. and Petsko, FEBS Lett., 203 (1986) 139.
38. a. Holdgate, G.A., Tunnicliffe, A., Ward, W.H.J., Weston, S.A., Rosenbrock, G., Barth, P.T., Taylor, I.W.F., Pauptit, R.A. and Timms, D., Biochem., 36 (1997) 9663.
    b. Hisler, V.J., Gomez, J. and Freire, E., Proteins Struct. Funct. Genet., 26 (1996) 123.